electronics

MDPI

Article

Design and Characterization of a Microwave Planar Sensor for Dielectric Assessment of Vegetable Oils

Aleksandr Ivanov [1,†], Timur Agliullin [1,†], Dario Laneve [2], Vincenza Portosi [2], Artem Vorobev [1], Raoul R. Nigmatullin [1], Aydar Nasybullin [1], Oleg Morozov [1], Francesco Prudenzano [2], Antonella D'Orazio [2] and Marco Grande [2,*]

1 Kazan National Research Technical University named after A.N. Tupolev-KAI, 10, Karl Marx st., Kazan 420111, Tatarstan, Russia; aleste1@mail.ru (A.I.); taagliullin@mail.ru (T.A.); vartems14@gmail.com (A.V.); renigmat@gmail.com (R.R.N.); aydar.nasybullin@mail.ru (A.N.); microoil@mail.ru (O.M.)

2 Dipartimento di Ingegneria Elettrica e dell'Informazione, Politecnico di Bari, Via E. Orabona, 4, 70125 Bari, Italy; dario.laneve@poliba.it (D.L.); vincenza.portosi@poliba.it (V.P.); francesco.prudenzano@poliba.it (F.P.); antonella.dorazio@poliba.it (A.D.)

* Correspondence: marco.grande@poliba.it

† These authors contributed equally to this work.

Received: 31 July 2019; Accepted: 11 September 2019; Published: 13 September 2019

Abstract: We report on the numerical simulations and experimental validation of a microwave planar sensor based on two coupled rings operating in the 4–6 GHz range. The fabricated sensor is used to characterize the dielectric permittivity of vegetable oils. We optimized the geometrical parameters in order to improve the overlap between the oil samples under study and the electric field. The experimental results showed an excellent match with the simulation results. The fabricated sensor allowed to retrieve the oil permittivity with a sensitivity of about 35 MHz per permittivity unit in the frequency range of interest. This paves the way to the realization of compact and sensitive sensors for a wide plethora of fields ranging from industry and food to chemistry and biology.

Keywords: dielectric constant measurement; microwave measurements; planar sensor; olive oil

1. Introduction

Microwave sensors have found wide application in industry, food, chemistry, biology, medicine, and other areas, where accurate measurements of the material concentration and dielectric permittivity is required in order to assess the quality of the substances [1]. Since the dielectric constant varies in microwave frequency range, the measurements are carried out in the frequency range where a strong variation is shown (this behavior usually happens at high frequencies). Depending on the type and volume of the sample under study, the methods for the dielectric constant measurement also differ, such as transmission-only, reflection-only, transmission–reflection, and resonant cavity methods [2–11]. The measurement techniques can be divided into two subgroups: resonant and nonresonant. Typically, nonresonant methods are useful for characterization of high- and medium-loss materials, and resonant methods can be used for measurements of materials with low losses. On the other hand, resonant techniques are in most cases limited to one fixed frequency (although sometimes a few different modes can be used in one measurement cell), while nonresonant methods can typically operate at broad frequency bands. One of the most important issues for all methods is their sensitivity to the presence of air gaps between the sample and other parts of the measurement cell. Resolution of loss tangent measurements for both resonant and nonresonant methods is associated with the presence of parasitic losses in measuring cells. Parasitic losses must be calculable and relatively small with respect to the sample losses in the sample in order to do precise measurements [11]. In case of resonant methods, the operating frequency range of the resonator is used, and the dielectric constant of the substance is determined by the change of the resonant frequency [12]. Resonant methods use various measurement media, for example, cavities, free space, metal waveguide, coaxial waveguide, strip lines, and so forth [13,14]. Sensors based on conventional waveguides and coaxial lines typically have larger size, they require a larger volume of test material for measurement, and their integration into electrical circuits is complicated. Therefore, methods using planar waveguides and microstrip lines have found the widest applications [15–17]. The additional advantages of planar sensors are the low-cost fabrication, the possibility to monitor in real time, as well as their nondestructive measurement nature [18].

In this paper, the design and the experimental characterization of a novel microwave planar resonator is illustrated. The coupling between two symmetric microstrip rectangular rings is exploited to increase the sensitivity of the resonator frequency to the dielectric properties of the several oils. In contrast to a single-square resonator design [19], in the proposed design a second resonance dip of the scattering parameter S_{11} arises due to the coupled rings configuration. The second resonance is characterized by a higher quality factor and a higher frequency shift when the dielectric constant of the tested substance varies, which in turn leads to a higher sensitivity. At the same time, the second resonance has higher field concentration at the center of the sensing area, which also increases the sensitivity of the sensor. The sensor proposed in the current work shows high sensitivity and Q-factor, which makes it suitable for the microwave characterization of liquids, such as vegetable oils with close values of permittivity [20]. In particular, we considered two types of olive oil and one type of sunflower oil, as well as their mixture at a concentration of 50%/50%.

2. Sensor Design and Simulations

The proposed sensor was modelled via the three-dimensional (3D) electromagnetic simulation software CST Microwave Studio (Dassault Systèmes Simulia, Providence, RI, USA). The geometrical parameters of the sensor are depicted in Figure 1a. The sensor is manufactured on Rogers 5880 substrate with relative permittivity ε_r = 2.2, thickness of 0.787 mm, and copper foil thickness of 35 µm.

Each oil sample to be characterized was placed in a plastic Petri dish, located on the top layer of the sensor. The Petri dish modelled in the simulations is identical to that used in the experiment, with a diameter of 35 mm, a thickness of 1 mm thick with an air gap on the bottom equal to 0.65 mm, and relative permittivity ε_r = 2.5.

Firstly, the gap between the T-structure of the feed line and the rectangular rings and the gap between the rectangular rings, along with the position of the Petri dish on the top layer of the sensor were optimized in order to improve the overlap between the oil sample and the electric field. In particular, the position of the Petri dish was chosen so that the oil sample is located in the region of maximum field concentration of the sensor. It was found that the optimal position is achieved when the center of the Petri dish is located at 34 mm from the feeding port. Then, the Petri dish was fixed in the optimal position. For this purpose, a support made of polylactide (PLA) plastic with permittivity of 3.5 was considered (grey region in Figure 1a). Figure 1b depicts the modulus of the simulated scattering parameter $|S_{11}|$ of the optimized configuration, in the frequency range of interest, which shows two resonant dips. The electric field distribution at the first resonance frequency, equal to 4.958 GHz is shown in Figure 2a, while the electric field distribution at the second resonance frequency, located at 5.652 GHz is shown in Figure 2b. The cross-section of the electric field in the middle of rectangles at the second resonance frequency is presented in Figure 2c. The amplitudes of the first and second resonance dips are −10.8 dB and −9.8 dB, respectively; the full widths at half minima (FWHMs) are 32.8 MHz and 11.9 MHz, respectively; the Q-factors are 151 and 572, respectively. Hereinafter, we will consider only the second dip, since it has significantly higher Q-factor and sensitivity (frequency shift per permittivity unit). This is justified by the total electric field distribution that is concentrated in the center of the sensor (i.e., across the gap between the coupled rings), as shown in Figure 2b.

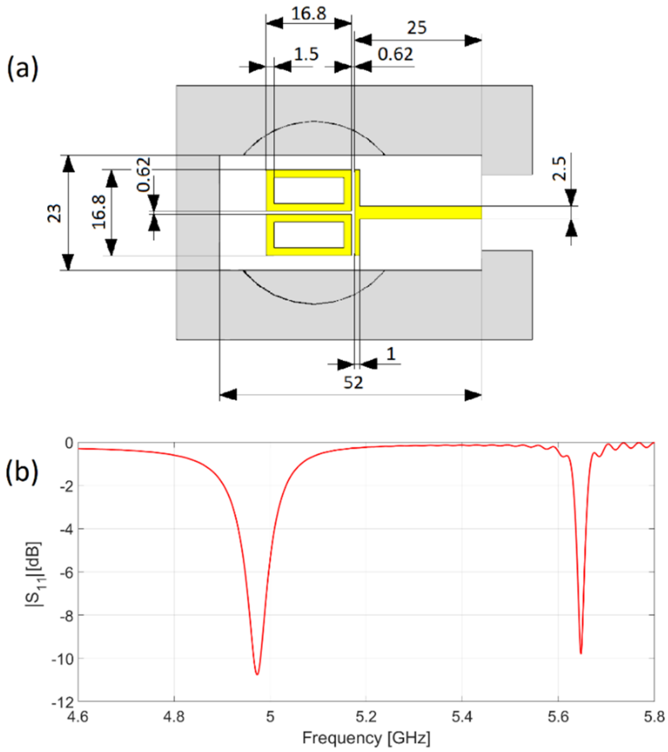

Figure 1. (**a**) Sketch of the top layer of the proposed sensor (all the geometrical parameters are in mm). (**b**) Modulus of the simulated scattering parameter $|S_{11}|$ of the sensor in air, supported by the PLA (polylactide) support (grey area) in the frequency range of interest.

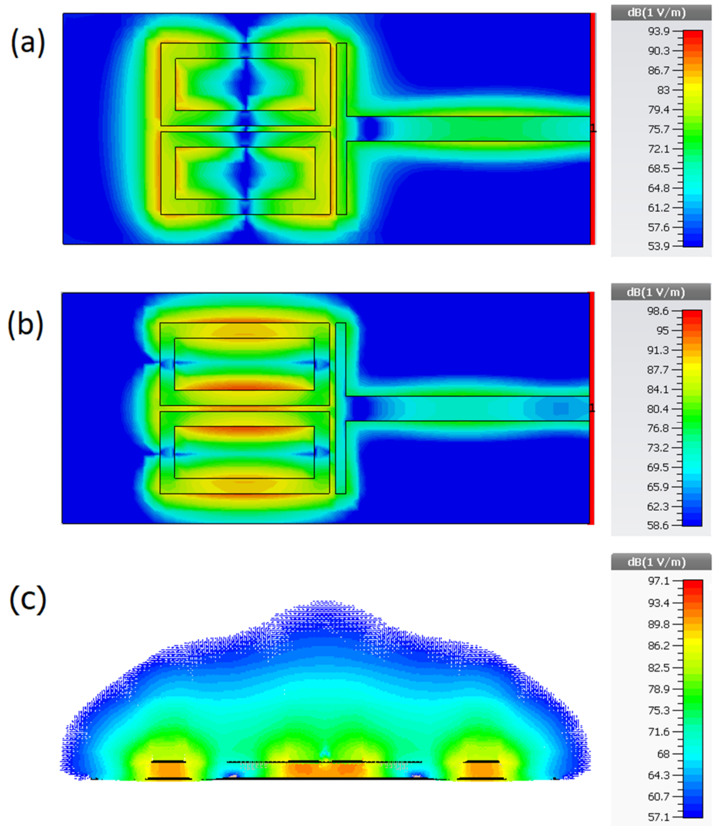

Figure 2. Total electric field distribution for (**a**) the first resonance at 4.958 GHz, (**b**) second resonance at 5.652 GHz, (**c**) transverse cross-section in the middle of ring resonators at 5.652 GHz.

It must be noted that the resonant frequency of the sensor mainly depends on the dimensions of the coupled rectangle structures, the distance between them, and the distance between rectangles and waveguide structure. Figure 3 illustrates the influence of the coupled structures width on the resonant frequency and Q-factor. The data are fitted using 3rd-order polynomials.

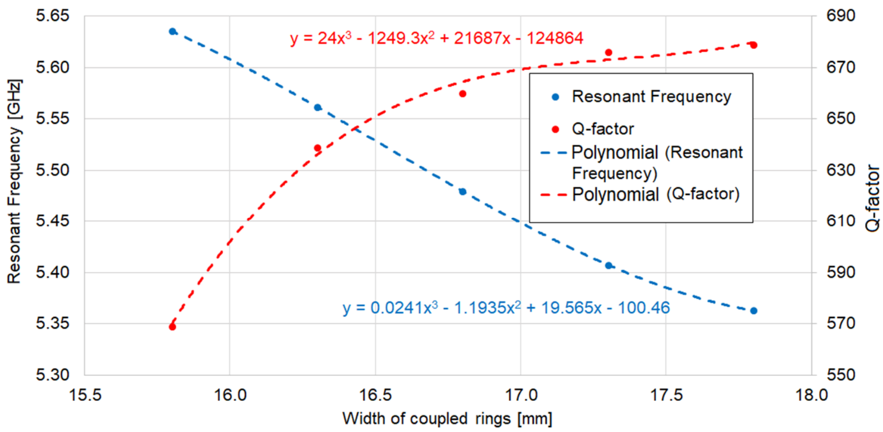

Figure 3. Influence of the coupled rings width on the resonant frequency and Q-factor.

Figure 4a shows the modulus of the simulated scattering parameter $|S_{11}|$ with and without an empty Petri dish located in the optimal position on the top layer of the sensor. It is worth highlighting that the introduction of the plastic Petri dish does not affect the resonances in terms of Q-factor. The Figure 4b shows the modulus of the simulated scattering parameter $|S_{11}|$ in the frequency range of interest when the Petri dish is filled (h = 8 mm) with a substance whose dielectric constant varies from 2.2 to 2.5. Table 1 shows the data of the numerical resonant frequencies. According to these results, there is a linear variation in the resonant frequency of the sensor, with a shift of $\Delta f = 3.5$ MHz in the frequency range of interest. That is, a high sensitivity of 35 MHz per permittivity unit can be achieved.

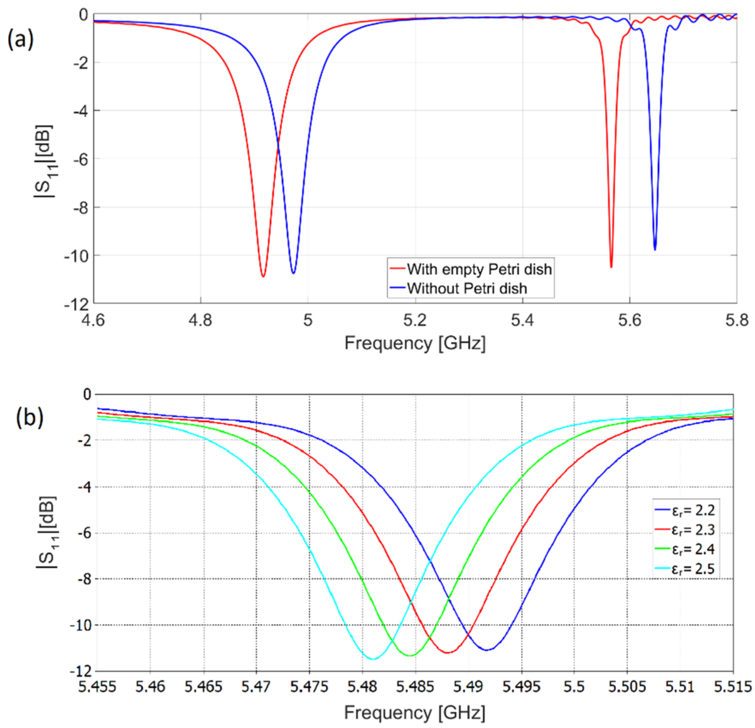

Figure 4. Modulus of the simulated scattering parameter $|S_{11}|$ of the sensor in the frequency range of interest with (**a**) empty Petri dish (red line) and no Petri dish (blue line), and (**b**) filled Petri dish at various permittivity ε_r of the substance. In both cases, the Petri dish is located in the optimal position.

Table 1. Simulated results pertaining to the second resonance when the substance permittivity was varied.

ε_r of Substance	Frequency, GHz
2.2	5.4917
2.3	5.4882
2.4	5.4847
2.5	5.4812

3. Experimental Results

In order to validate the numerical predictions, we fabricated the proposed microwave sensor by means of the Printed Circuit Board (PCB) prototyping system LPKF ProtoLaser U3 (PLU3). The PLU3 is based on a frequency-tripled Nd:YAG diode laser emitting at 355 nm, used for copper etching. The PLU3 has a resolution of 2 µm, which is very suitable for fabricating microwave devices. The plastic support was manufactured in PLA using 3D printing technology to accommodate the plastic dishes with a 35 mm diameter. Figure 5a illustrates the experimental setup with the fabricated sensor, while the modulus of the scattering parameter $|S_{11}|$ of the sensor with and without an empty Petri dish is shown in Figure 5b. The measured $|S_{11}|$ spectrum shown in Figure 5b is in excellent agreement with the simulated $|S_{11}|$ spectrum shown in Figure 4a, the difference between the two $|S_{11}|$ plots is in the order of few MHz.

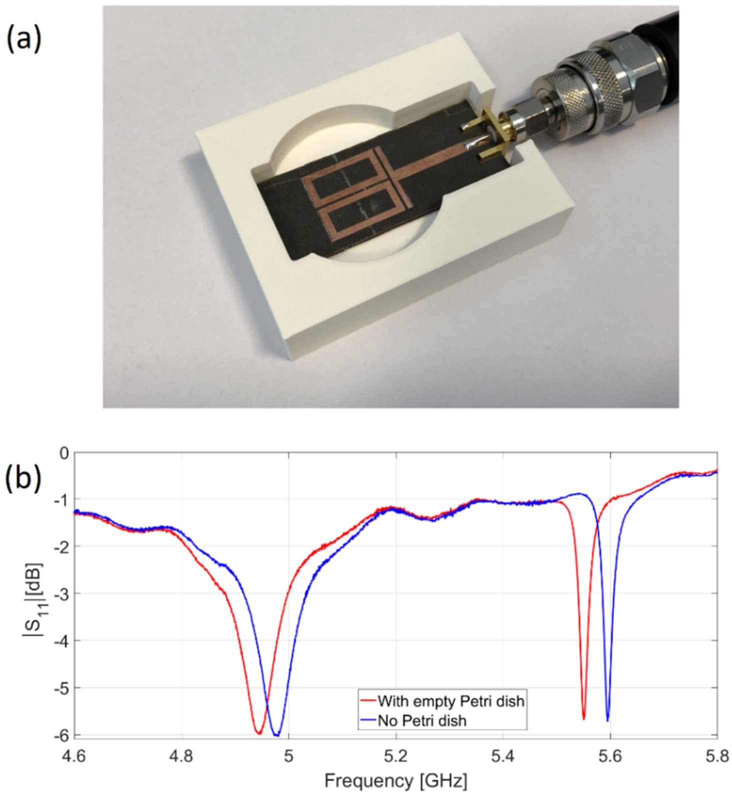

Figure 5. (**a**) Experimental setup. (**b**) Modulus of the measured scattering parameter $|S_{11}|$ of the sensor with no Petri dish (blue line) and an empty Petri dish, placed in the optimum position by means of the plastic PLA support (red line).

Firstly, we calibrated the proposed sensor by filling the Petri dish with an 8 mm level of a reference liquid (isopropanol, IPA @ 25 °C) that showed an experiential resonance at 5.441 GHz. This value compares very well with the simulated value, equal to 5.443 GHz when a complex permittivity is considered (ε = 3.43 + j1.5) [21]. This shift leads to an average sensitivity of about 43 MHz per permittivity unit (leading to a difference of the relative permittivity $\Delta\varepsilon_{real} = \varepsilon_{real\_IPA} - \varepsilon_{real\_air} = 2.43$).

To measure and determine the sensitivity of the fabricated sensor, two types of extra-virgin olive oil and one type of sunflower oil were considered, and measurements of single oils and their mixture (at a concentration of 50%/50%) were carried out. Figure 6a shows the frequency shift of the measured $|S_{11}|$ spectrum of the sensor when the Petri dish is filled with 8 mm level of sample liquids, namely the two types of extra-virgin olive oils (A and B) and their 50/50 mixture. It is worth stressing that we used the same plastic Petri dish for all the measurements. The solid lines refer to the experimental data acquired by means of a Vector Network Analyzer (VNA, Agilent Technologies N9917A) in the frequency range 5.479–5.506 GHz. The experimental data were fitted by means of a MATLAB script that implements a 4th-order polynomial function, in order to define the minima. Figure 6b shows the frequency shift of the measured $|S_{11}|$ spectrum of the sensor when the Petri dish is filled with an 8 mm level volume sample of the extra-virgin olive oil A, the sunflower oil, and their 50/50 mixture. Also in this case, the experimental curves were fitted by means of a 4th-order polynomial function, to find the minima. The first column of Table 2 reports the experimental minima and their comparison for the first and second measurements. We retrieved the permittivity of the single oils by considering the linear dependence of the resonant frequency, shown in Figure 4. The fitting function between dielectric constant of the tested sample and the resonant frequency (f [GHz]) is formulated as follows: $\varepsilon_r = -23.131f + 129.38$.

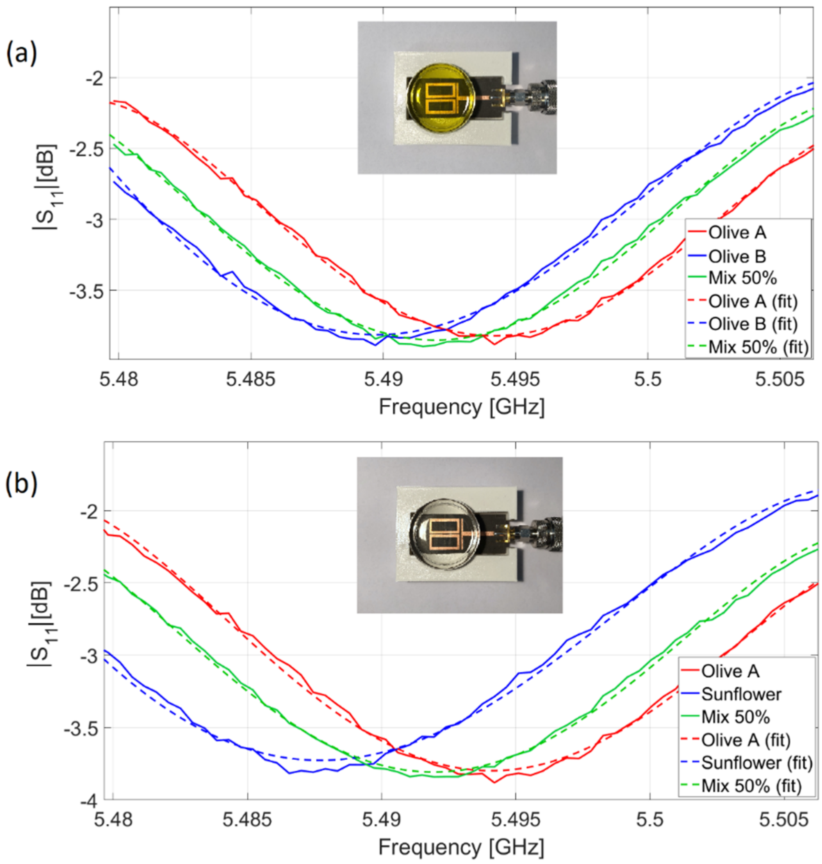

Figure 6. Modulus of the measured scattering parameter $|S_{11}|$ along with fitting curves for various oils and their mixtures: (**a**) Extra-virgin olive oil A vs. Extra-virgin olive oil B. (**b**) Extra-virgin olive oil A vs. Sunflower oil. Insets: Petri dish filled with (**a**) extra-virgin olive oil A and (**b**) sunflower oil.

These data allowed to determine the experimental sensitivity of the proposed microwave sensor that is equal to 35 MHz per permittivity unit in the frequency range of interest (around 5.5 GHz).

Table 2. Experimental data pertaining to the dielectric characterization of various oils and their mixtures.

Oil Sample	Minima Freq., GHz	Retrieved/Estimated ε_r
Olive A	5.4942	2.294
Olive B	5.4897	2.398
Sunflower	5.4878	2.442
Mix A–B	5.492	2.345
Mix A–Sunflower	5.4918	2.349

In Table 3, we compared the obtained results with some recently proposed microwave planar sensors in terms of sensitivity, frequency range, and Q-factor. By observing the Table 3, the very good sensitivity of the proposed microwave planar sensor is apparent.

Table 3. Comparison between the proposed sensor and recently reported researches.

Reference	Sensor Type	Sensitivity MHz/Permittivity Unit	Resonant Frequency	Q-Factor
[19]	Rectangular ring resonator	25.7 MHz (avg)	3.992 GHz	174
[22]	Multiple split-ring resonator	0.75–1 MHz	2.121 GHz	525
[23]	Symmetrical split-ring resonator with double spurlines (only solids—2 port systems)	33.5 MHz (avg)	2.22 GHz	653
Proposed sensor	Rectangular double-ring resonator	43 MHz (exp. avg)/ 35 MHz at 5.5 GHz	5.652 GHz	~572 (sim. empty Petri dish) ~230 (exp. empty Petri dish)

4. Discussion and Conclusions

In this paper, we presented a microwave planar sensor for the measurement of the dielectric constant of liquids and specifically, of vegetable oils operating in the 4–6 GHz frequency range. In particular, we proposed two coupled symmetric rectangular rings, which resulted in two resonant modes. We optimized the geometrical parameters, taking into account the presence of vegetable oils in a plastic Petri dish, whose position on the sensor top layer is optimized. Numerical results showed that the second resonance has significantly higher Q-factor and sensitivity (i.e., frequency shift per permittivity unit). The proposed microwave sensor was fabricated by means of the PCB prototyping system LPKF ProtoLaser U3 (PLU3). The experimental results fully confirm the numerical analysis, showing the possibility to identify different types of vegetable oils. It is worth stressing that our approach was successful in distinguish two different kinds of extra-virgin oils that have similar optical properties to the naked eye. The sensor also showed good sensitivity in dielectric constant measurement of olive oil mixing products. The achieved sensitivity of the fabricated sensor is 35 MHz per permittivity unit at 5.5 GHz (while the average sensitivity is about 43 MHz per permittivity unit when the reference liquid IPA is considered). The experimental Q-factor of the fabricated sensor is about 232. These results compare very well/overcome the performance of the recently reported microwave planar sensors. One of the options for further work is to improve the sensor performance by introducing the Fano resonance, which has narrower resonance peak, resulting in higher Q-factor.

These promising results pave the way for the realization of compact and sensitive biological/chemical microwave sensors that could find application in a wide plethora of fields such as industry, food, chemistry, biology, medicine, and other areas, where accurate measurements of the dielectric properties are required.

Author Contributions: A.I. and T.A. performed the numerical simulations. D.L., V.P. and F.P. fabricated the sensor. A.I., T.A. and M.G. integrated the sensor and performed the experiments. M.G. supervised the work. A.I. and T.A. drafted the manuscript. A.I., T.A., D.L., V.P., A.V., R.R.N., A.N., O.M., F.P., A.D. and M.G. commented, edited and reviewed the manuscript.

Funding: This work is partially performed as a part of the state task (base part of program "Asymmetry" 8.6872.2017 and project part of program «Sokol» No 2.1724.2017/4.6) which is carried out by Kazan National Research Technical University named after A.N. Tupolev-KAI (KNRTU-KAI).

Conflicts of Interest: The authors declare no conflict of interest.

References

1. Chen, L.F.; Ong, C.K.; Neo, C.P.; Varadan, V.V.; Varadan, V.K. *Microwave Electronics: Measurement and Materials Characterization*, 1st ed.; John Wiley & Sons: Hoboken, NJ, USA, 2004.
2. Liu, W.; Sun, H.; Xu, L. A microwave method for dielectric characterization measurement of small liquids using a metamaterial-based sensor. *Sensors* **2018**, *18*, 1438. [CrossRef] [PubMed]
3. Zhao, C.; Jiang, Q.; Jing, S. Calibration-independent and position-insensitive transmission/reflection method for permittivity measurement with one sample in coaxial line. *IEEE Trans. Electromagn. Compat.* **2011**, *53*, 684–689.
4. Haase, N.M.N.; Fuge, G.; Trieu, H.K.; Zeng, A.; Jacob, A.F. Miniaturized transmission-line sensor for broadband dielectric characterization of biological liquids and cell suspensions. *IEEE Trans. Microw. Theory Tech.* **2015**, *63*, 3026–3033. [CrossRef]
5. Patricia, L.R.; David, E.B.; David, P.M.; Frank, W. Comparison of metal-backed free-space and open-ended coaxial probe techniques for the dielectric characterization of aeronautical composites. *Sensors* **2016**, *16*, 967.
6. Liu, W.; Xu, L.; Yang, X.; Shi, Y.; Zhan, H. Complex permittivity determination based on a radio frequency device. *Sens. Actuators A Phys.* **2018**, *272*, 75–82. [CrossRef]
7. Reinecke, T.; Hagemeier, L.; Spehlbrink, H.; Guenther, S.; Klintschar, M.; Zimmermann, S. Open-ended coaxial probe for the quantification of edema in human brain tissue. *Sens. Actuators B Chem.* **2014**, *204*, 763–769. [CrossRef]
8. Ocera, A.; Dionigi, M.; Fratticcioli, E.; Sorrentino, R. A novel technique for complex permittivity measurement based on a planar four-port device. *IEEE Trans. Microw. Theory Tech.* **2006**, *54*, 2568–2575. [CrossRef]
9. Janezic, M.D.; Williams, D.F.; Blaschke, V.; Karamcheti, A. Permittivity characterization of low-k thin films from transmission-line measurements. *IEEE Trans. Microw. Theory Tech.* **2003**, *51*, 132–136. [CrossRef]
10. Liu, C.; Pu, Y. A microstrip resonator with slotted ground plane for complex permittivity measurements of liquids. *IEEE Microw. Wirel. Compon. Lett.* **2008**, *18*, 257–259.
11. Krupka, J. Frequency domain complex permittivity measurements at microwave frequencies. *Meas. Sci. Technol.* **2006**, *17*, 55–70. [CrossRef]
12. Hinojosa, J.; Lmimouni, K.; Lepilliet, S.; Dambrine, G. Very high broadband electromagnetic characterization method of film-shaped materials using coplanar waveguide. *Microw. Opt. Technol. Lett.* **2002**, *33*, 352–355. [CrossRef]
13. Hippel, A.V. *Dielectric Materials and Applications*; Artech House: Norwood, MA, USA, 1995.
14. Hippel, A.V. *Dielectrics and Waves*; Artech House: Norwood, MA, USA, 1995.
15. Ganchev, S.I.; Qaddoumi, N.; Bakhtiari, S.; Zoughi, R. Calibration and measurement of dielectric properties of finite thickness composite sheets with open-ended coaxial sensors. *IEEE Trans. Instrum. Meas.* **1995**, *44*, 1023–1029. [CrossRef]
16. Hasar, U.C. Permittivity determination of fresh cement-based materials by an open-ended waveguide probe using amplitude-only measurements. *Prog. Electromagn. Res.* **2009**, *97*, 27–43. [CrossRef]
17. Huang, R.; Zhang, D. Application of mode matching method to analysis of axisymmetric coaxial discontinuity structures used in permeability and/or permittivity measurement. *Prog. Electromagn. Res.* **2007**, *67*, 205–230. [CrossRef]
18. Queffelec, P.; Gelin, P. Influence of higher order modes on the measurements of complex permittivity and permeability of materials using a microstrip discontinuity. *IEEE Trans. Microw. Theory Tech.* **1996**, *44*, 816–824. [CrossRef]

19. Alahnomi, R.; Hamid, N.B.A.; Zakaria, Z.; Sutikno, T.; Mohd Bahar, A. Microwave planar sensor for permittivity determination of dielectric materials. *Indones. J. Electr. Eng. Comput. Sci.* **2018**, *11*, 362–371. [CrossRef]
20. Nigmatullin, R.R.; Vorobev, A.S.; Nasybullin, A.R.; D'Orazio, A.; Maione, G.; Lino, P.; Grande, M. Advanced and sensitive method by discrete geometrical invariants for detection of differences between complex fluids. *Commun. Nonlinear Sci. Numer. Simul.* **2019**, *73*, 265–274. [CrossRef]
21. Gregory, A.P.; Clarke, R.N. *Tables of the Complex Permittivity of Dielectric Reference Liquids at Frequencies up to 5 GHz*; National Physical Laboratory Report; National Physical Laboratory: Teddington, UK, 2012.
22. Mohd Bahar, A.; Zakaria, Z.; Ab Rashid, S.; Isa, A.; Alahnomi, R. Dielectric analysis of liquid solvents using microwave resonator sensor for high efficiency measurement. *Microw. Opt. Technol. Lett.* **2017**, *59*, 367–371. [CrossRef]
23. Alahnomi, R.; Zakaria, Z.; Ruslan, E.; Ab Rashid, S.; Mohd Bahar, A. High-Q sensor based on symmetrical split ring resonator with spurlines for solids material detection. *IEEE Sens. J.* **2017**, *17*, 2766–2775. [CrossRef]